
Article:
Jana, Kamalesh, Blackman, David R., Shaikh, Moniruzzaman et al. (6 more authors) (2018) Probing ultrafast dynamics of solid-density plasma generated by high-contrast intense laser pulses. Physics of Plasmas. 013102. ISSN 1089-7674

https://doi.org/10.1063/1.5005176

Probing ultrafast dynamics of solid-density plasma generated by high-contrast intense laser pulses

Kamalesh Jana[1], David R. Blackman[2], Moniruzzaman Shaikh[1], Amit D. Lad[1], Deep Sarkar[1], Indranuj Dey[1], Alex P.L. Robinson[3] John Pasley[2] and G. Ravindra Kumar[1]*

[1] *Tata Institute of Fundamental Research, Dr. Homi Bhabha Road, Colaba, Mumbai-400005, India*

[2] *York Plasma Institute, University of York, Heslington, York YO10 5DQ, United Kingdom and*

[3] *Central Laser Facility, Rutherford-Appleton Laboratory, Chilton, Didcot OX11 0QX, United Kingdom*

(Dated: November 27, 2017)

We present ultrafast dynamics of solid-density plasma created by high-contrast (picosecond contrast $\sim 10^{-9}$), high-intensity ($\sim 4 \times 10^{18}$ W/cm^2) laser pulses using time-resolved pump-probe Doppler spectrometry. Experiments show a rapid rise in blue-shift at early time delay (2 ps-4.3 ps) followed by a rapid fall (4.3 ps-8.3 ps) and then a slow rise in blue-shift at later time delays (>8.3 ps). Simulations show that the early-time observations, specifically the absence of any red-shifting of the reflected probe, can only be reproduced if the front surface is unperturbed by the laser pre-pulse at the moment that the high intensity pulse arrives. A flexible diagnostic which is capable of diagnosing the presence of low-levels of pre-plasma formation would be useful for potential applications in laser-produced proton and ion production, such as cancer therapy and security imaging.

I. INTRODUCTION

The advent of high power, femtosecond lasers has made study of laser-plasma interaction more accessible in the laboratory[1–3]. When an ultraintense, femtosecond laser pulse interacts with solid matter, it produces high temperature, near-solid density, plasma[1,2]. Understanding the physics of the laser-plasma interaction process is very important not only for the study of extreme states of matter but also for the development of table-top X-ray and THz sources and novel sources of electrons, ions and positrons[1,4–7]. The hot, dense plasma created via different laser absorption mechanisms[8,9] evolves on an ultrafast timescale. It is very important to know the temporal evolution of the plasma density profile during a laser-plasma interaction in order to gain a better understanding of the interaction process[2,10].

Very little work has so far been done to explore ultrafast plasma dynamics[11–13] in the relativistic intensity regime (>10^{18} W/cm^2). At relativistic intensity, the main femtosecond pulse is typically preceded by a longer pre-pulse[14], which is intense enough to create a pre-plasma at the target front-surface. So, intensity contrast (ratio of pre-pulse intensity to main-pulse intensity) is an important parameter in laser-matter interactions. Nowadays, laser intensity contrast has been improved significantly[14–16]. Many experiments carried out with lower contrast lasers have been revisited with improved higher contrast laser pulses[15–19] but study of ultrafast laser-plasma dynamics with higher contrast pulses is mostly unexplored. Previous studies of ultrashort laser-plasma dynamics at relativistic intensity have been performed with comparatively low-contrast lasers[12,13]. With a higher contrast laser the interaction process is expected to be modified significantly due to the reduction in pre-plasma formation, since the previously observed dynamics takes place in the pre-plasma region. For this reason studying laser-plasma interaction hydrodynamics using these cleaner (higher contrast) pulses is crucial to gaining a comprehensive understanding of high intensity, short-pulse laser induced plasma dynamics.

In this paper, we report pump-probe Doppler spectroscopy experiment carried out with a high contrast (ps contrast$\sim 10^{-9}$) laser at relativistic intensity ($\sim 4 \times 10^{18}$

*Electronic address: grk@tifr.res.in

W/cm^2). Here the plasma is created by an 800 nm, 30 fs pump pulse focused onto an Al-coated BK-7 target. A time-delayed second harmonic (400 nm) pulse is used to probe the plasma. The second harmonic probe reflects from its critical surface ($n_e \sim 6 \times 10^{21}$cm^{-3}) in, what is for the pump beam, over-dense plasma. The Doppler shifts recorded at this surface at various times after the arrival of the pump pulse serve to illustrate the hydrodynamic evolution of the plasma. Time-resolved Doppler-shift data show rapid outward motion of the probe critical layer at early time delays (2 ps-4.3ps). After that the motion slows down rapidly (4.3 ps-8.3 ps) before increasing again at a slower rate. Simulation results show that the behaviour observed can only manifest in the case where target remains unperturbed by the laser pre-pulse. On the other hand, the presence of pre-plasma correlates with observations of red-shifting at early times, such as have been previously reported[12,13]. This suggests possible applications in on-shot detection of pre-plasma formation that is more flexible than the side-on imaging techniques that are typically employed. The sensitivity of this diagnostic is demonstrated here by the performance of a simulation with severely limited pre-plasma evolution and its comparison with a simulation in which there is no pre-plasma at all. Comparing pseudo-diagnostic output for these two cases still results in a switching from red-to-blue-shift (with limited pre-plasma) to blue-shift-only data (with no pre-plasma), thereby supporting our suggestion that this diagnostic is able to distinguish effectively between cases in which there is limited pre-plasma evolution and cases in which there is none. Whilst side-on optical shadowgraphy and interferometry have traditionally been employed to diagnose pre-plasma formation[20], there are severe constraints on the use of these techniques: only convex and small planar surfaces can be diagnosed. The use of more extended planar surfaces results in horizon problems, often partly due to the fact that it is difficult to align the imaging axis with sufficient angular precision relative to the target surface. Concave surfaces are impractical except where the plasma extends at high density far from the interaction point of the main pulse. Some experiments require low levels of pre-plasma formation in a geometry that is inaccessible to an optical probe that comes in parallel to the interaction surface. Proton fast-ignition for inertial confinement fusion (ICF) is one such example[21]. High-efficiency production of protons usually relies upon the interaction of an extremely high contrast laser pulse with a thin foil target[22]. Since the proton production foil in proton fast-ignition is located near the tip of the interior of a hollowed out cone, which itself is inserted into the side of an ICF capsule, the use of side-on probing is completely ruled out. Laser-produced proton/ion experiments with applications to medical or security imaging[23] are also likely to employ geometries that render side-on diagnosis of low-level pre-plasma formation challenging. For this reason a diagnostic technique that can interrogate pre-plasma formation using a target surface normal, or oblique, probe beam has potential value for applications where on-shot diagnosis of pre-plasma formation is important for proper functioning. The technique described here is sensitive to even very small quantities of pre-plasma formation, such as may be critical to such experiments, and is amenable to either target surface normal or oblique probing geometries. Furthermore the relatively low-cost and robustness of all elements of this diagnostic make it attractive for such applications.

It is interesting to compare our technique with others prevalent in studies of rapid plasma dynamics and shocks in condensed phase targets. VISAR (velocity interferometer system for any reflector)[24] proposed in 1972, is a well-established and widely practised technique for studying target surface motion in particularly shocks. It gives spatial and temporal information of the velocity evolution at a target surface. The spatial resolution is determined by the magnitude of the fringe shift in the interferometer, the temporal resolution by the streak camera used for detection. The spatial resolution can be very high, depending on the wavelength of the laser used, the temporal resolution, however, is limited by the streak camera (typically picosecond to tens of picosecond)[25]. Chirped pulse reflectivity and frequency domain interferometry adapted from radar technology[26] is an innovative technique where the time domain information of shock

propagation is encoded into the frequency of a chirped probe laser pulse[27]. The probe pulse has a specific, predetermined arrangement of wavelengths with respect to time within the pulse itself. Each wavelength therefore, offers a measurement of the velocity at a specific time point and the evolution of the shocked target can be obtained using a single chirped probe pulse. It is, however, important to know the temporal shape of the input pulse using complete pulse characterization techniques like FROG (frequency resolved optical gating)[29] or SPIDER (spectral phase interferometry for direct electric-field reconstruction)[28]. Also, the wavelength needs to be measured with high resolution to ensure high temporal resolution. The spatial resolution is again limited by the wavelength used and the probe focusing conditions.

The pump-probe Doppler spectrometry that we use in this paper can have very high temporal resolution (tens of femtosecond), limited only by the duration of the probe pulse (the time delay steps offered by the translation stage can easily be in the few femtosecond range and are therefore not a constraint). We present spatially integrated measurements in this paper. One can, however, envisage obtaining spatially resolved measurements by moving the focused probe beam across the target surface from shot-to-shot or using multichannel detection of light reflected from distinct points in a single laser shot. This technique is simpler than VISAR as it does not use an interferometric set up and time resolution is not limited by the detector but is instead selected based on the requirements of the experiment and the number of shots that are realistically available to cover the time-window of interest.

II. EXPERIMENT

Figure 1(a) shows the schematic of the experimental setup. The experiment was performed at the Tata Institute of Fundamental Research (TIFR), Mumbai using a chirped pulse amplification based Ti: Sapphire 100 TW laser system which can deliver 800 nm, 30 fs pulses at 10 Hz repetition rate. The picosecond intensity contrast of the laser pulse was $\sim 10^{-9}$ (shown in figure 1(b)). The main pump beam was focused by an f/4 off-axis parabolic mirror to a 35 μm, focal spot (FWHM) on an optically polished ($\lambda/10$) BK-7 glass target at a 45° angle of incidence. The peak intensity was $\sim 4 \times 10^{18}$ W/cm^2. A motorized high-precision stage was used to move the target so that every laser pulse interacted with a fresh position on the target. A small fraction of the main laser beam was extracted and up-converted to its second harmonic (400 nm) by β-barium borate (BBO) crystal and used as the probe pulse. A BG-39 filter was used after the BBO crystal to remove the residual 800 nm light in the probe. The probe was focused onto the plasma at normal incidence to a 120 μm focal spot (FWHM). The probe intensity was kept low ($\sim 4 \times 10^{10}$ W/cm^2) so that it did not ionize the target. Spatial overlap between the pump and the probe beams was ensured by high resolution imaging. The probe beam was time-delayed with respect to the pump beam using a high precision motorized retro-reflector delay stage. The reflected probe was collected by a lens and then split into two parts. One part went to a high-resolution (0.35Å) spectrometer (OOI, HR-2000) to record a spectrum at each time delay. The other part of the beam was fed to a photodiode (PD) which measured probe reflectivity at each time delay. Temporal overlap between the pump and the probe beams was monitored by observing probe reflectivity as function of probe time-delay. When the probe arrives at the target surface before the pump (negative time delay), it is reflected from a cold target and gives high reflectivity. If the probe arrives simultaneously with pump beam, it is then reflected from plasma created by pump and there is a reduction in probe reflectivity due to plasma absorption. The delay at which there is a sudden transition in probe reflectivity is called time zero.

III. RESULTS AND DISCUSSION

Doppler spectrometry relies upon measuring quantitative wavelength shifts in probe light that has reflected from the plasma created by pump laser. Figure 2(a)

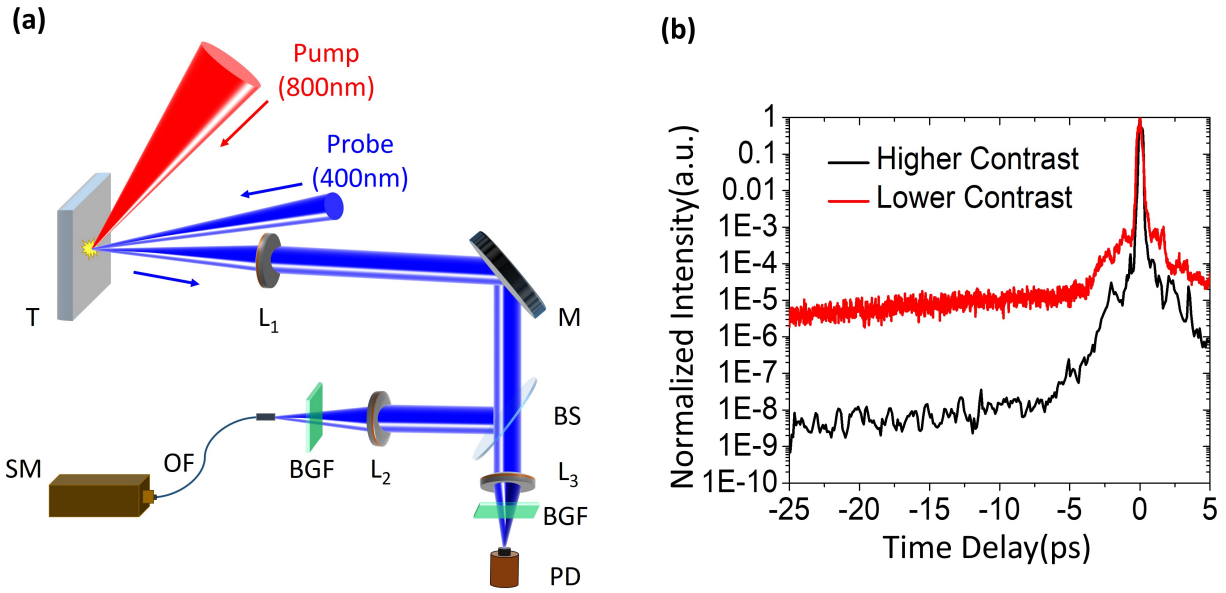

FIG. 1: (a) **Schematic of the experimental setup;** T:target(Al-coated BK-7 glass), M:mirror, $L_1 - L_3$:focusing lenses, BS:beam splitter, PD:photo-diode, SM:spectrometer, OF:optical fiber, BGF:Blue-green (BG-39) Filter. (b) Laser Intensity contrasts measured by a third-order cross-correlator (SEQUOIA). Picosecond intensity contrasts were $\sim 10^{-9}$ and $\sim 10^{-5}$ for higher (used in present experiment) and lower (used in earlier experiment by S. Mondal *et al.*[12]) contrast lasers respectively.

shows three normalized reflected probe spectra at different time delays for comparison. These show a very small red-shift and blue-shift compared to the reference spectrum (measured at zero delay) at 1.3 ps and 4.3 ps respectively. In order to measure the small wavelength shifts more accurately, the normalized reference spectrum is subtracted from all of the time delayed reflected spectra (normalized) and each curve is referred to as a difference amplitude curve (some such are shown in figure 2(b)). For a blue-shift, the difference amplitude changes its sign from positive to negative and vice versa for a red-shift. Doppler shifts were calculated by subtracting the central wavelength of the reference spectrum from that of the reflected probe spectra at each time delay. Time-resolved Doppler shift data (in figure 3(a)) show that there is a very small red-shift at early time followed by a rapid rise in blue-shift, a rapid fall and another rise at longer time delay. The velocity of probe-critical layer (V_{cr}) for a normally incident probe is related to the Doppler shift by the following relationship[30]

$$V_{cr} = -\ 0.5c\Delta\lambda/\lambda$$

Where λ is the incident probe wavelength and $\Delta\lambda$ is the Doppler shift. The velocity of the probe-critical surface as a function of probe time delay is shown in figure 3(b). Here negative (red-shift) and positive (blue-shift) velocity indicate inward and outward motion of the probe-critical surface respectively. At early time there is a very small inward motion. At $\sim$ 2 ps the velocity of the critical surface changes its sign and the velocity also increases rapidly. At $\sim$ 4.3 ps outward motion reaches its maximum velocity of 1.3×10^7 cm/s, which is then followed by a rapid decrease and then, later on, by a gradual increase in its magnitude. The experiment was carried out also at lower intensity ($\sim 7 \times 10^{17}$ W/cm^2) showing similar trends (insets of figure 3(a) and 3(b)). The small inward motion at early time may be caused by flow in some very limited pre-plasma, much like that observed in experiments performed at lower contrast, the alternative explanation being that the dense target surface is momentarily pushed inward. It is not trivial to distinguish between these two explanations since the radiation-hydrodynamic simulations are unable to precisely deter-

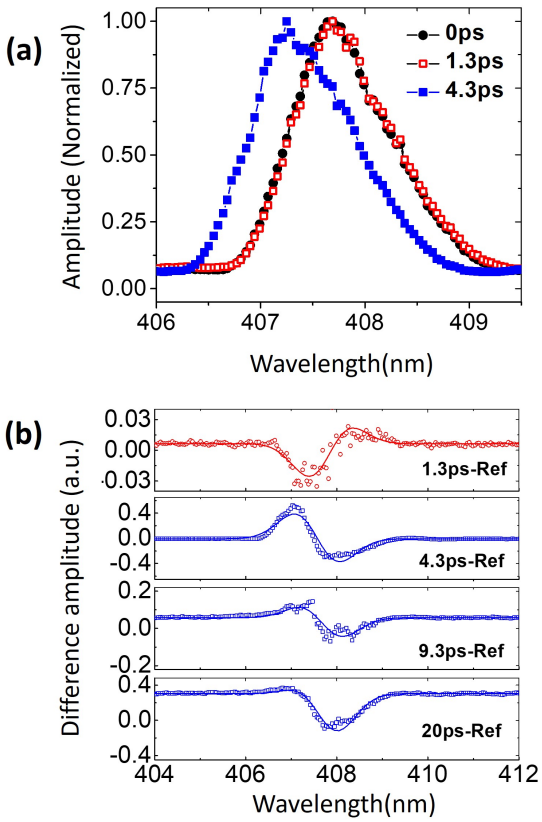

FIG. 2: (a) Normalized spectra of the reflected probe at different time delays. (b) Difference amplitudes at different probe delays.

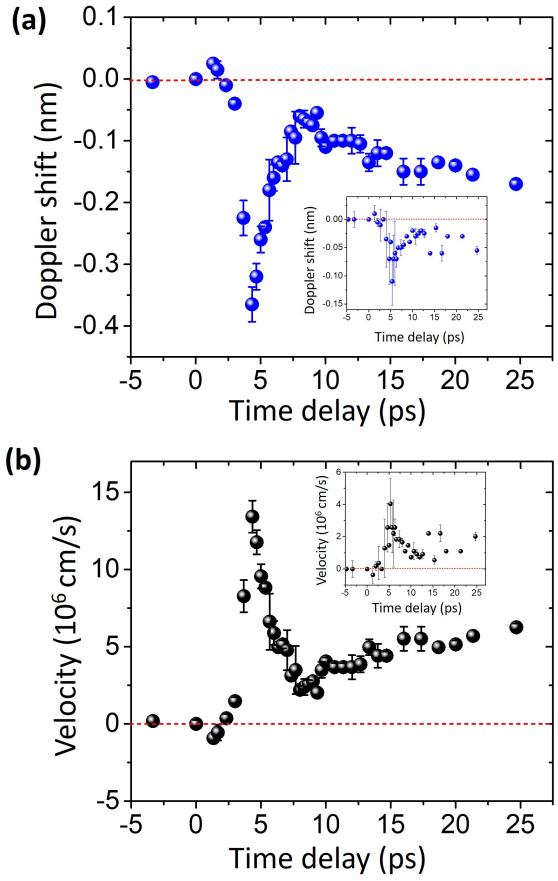

FIG. 3: (a) Time dependent Doppler shifts in reflected probe spectra (inset shows the same at lower intensity). (b) Velocities of probe-critical layer calculated from Doppler shifts (inset shows the same at lower intensity).

mine the point at which a target will start to ablate and form plasma, and such small quantities of pre-plasma are not readily diagnosed experimentally.

This result is quite different from the results obtained in earlier studies in the relativistic regime, where initially a large inward motion of the probe critical surface has been observed[12,13]. Those experiments were done using lower contrast lasers. In figure 4 our result is compared with the result obtained in the earlier experiment with lower contrast ($\sim 10^{-5}$) laser at almost the same intensity by S. Mondal *et al.*[12]. Because of the lower intensity contrast the pre-pulse of pump laser creates a pre-plasma and a shock-like disturbance is then generated in this pre-plasma which then propagates into the target. Thus, at early time, a large red shift is observed correlating to the motion of the shock-like disturbance into the target.

In the current experiment using a higher contrast laser there is no significant pre-plasma formation at the target surface. The absence of pre-plasma at the target surface prevents significant motion of the probe critical surface into the target.

IV. SIMULATIONS

1-D collisional particle in cell (PIC) simulations using EPOCH[31] have been performed of the target front surface interaction with the laser. These calculations employed an initial 2×10^8 particles in 25000 cells with a box size of 15 μm, and were run on 1200 cores. These calculations included both collisions and ionisation. The

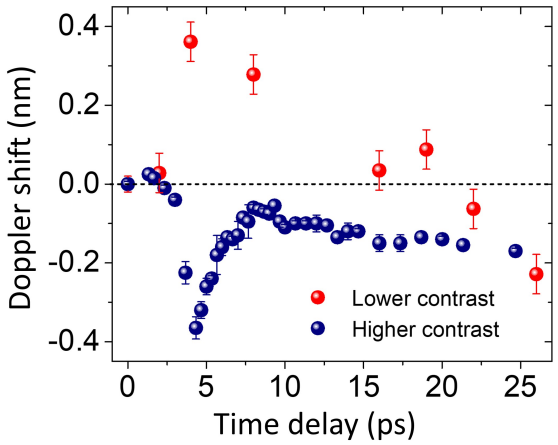

FIG. 4: Time resolved Doppler shift data (of present experiment) is compared with the data obtained at lower contrast laser experiment at same intensity (S. Mondal *et al.*[12]) .

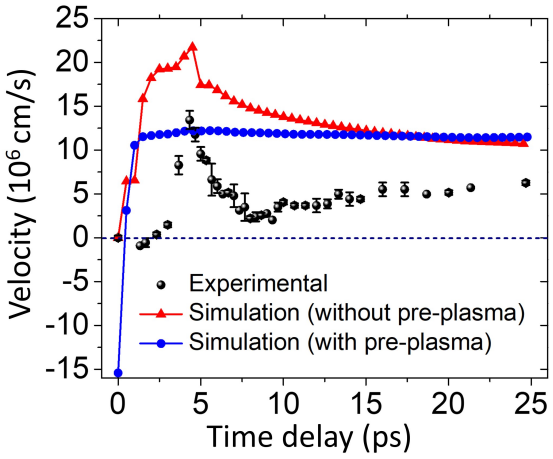

FIG. 5: Comparison of velocity of probe-critical surface found in the numerical simulation with experimental observation.

results of these calculations were used to initialise a 1-D hydrodynamics simulation that enables the evolution of the probe critical surface to be modelled over a duration that enables comparison with the experiment. For the initial front surface both step-like (unablated) and more gradually rising density profiles were investigated. Figure 5 shows a comparison of simulation results from a step-like front surface configuration with those from a simulation in which the front surface rises gradually to peak density over a distance of 1 micron. The latter being a test-case in which there is severely limited pre-plasma evolution as opposed to a profile that is predicted on the basis of the laser profile in the experiment.

It was demonstrated that the absence of the early time motion of the critical surface into the target is associated with the absence of pre-plasma formation at the target front surface. Only the calculations run using an assumption of a step-like initial front surface displayed comparable results. Other simulations, in which the plasma density rose gradually, inevitably displayed some inward directed motion of the critical surface at early times. The change in dynamics from the previous studies in which the critical surface moved inward at early times, corresponding to an inward propagating shock-like disturbance, can be readily understood. In absence of the pre-plasma the high density of the entirety of the target material precludes an inward propagating critical surface except in the case where the entirety of the target moves away from the laser. Such behaviour is not possible at these intensities. What is actually observed therefore is the explosive expansion of the initially unperturbed front surface of the target- an outward expansion as observed by the probe, which becomes less vigorous as time progresses due to the absence of further energy input. The small delay in the peaking of the critical surface velocity can be explained by the acceleration of material from an initially almost stationary configuration. It was found that in order to approach the relatively low velocities observed in the experiment the intensity of the laser had to be reduced by a factor of four. This may be explained partly by the fact that the probe is sampling plasma being illuminated at a range of intensities and also by the fact that in the experiment the expansion will not be one-dimensional, but rather will have a strongly two dimensional nature that will tend to limit the on-axis velocities substantially by comparison with the 1-D case. Furthermore PIC calculations tend to over-estimate temperatures, which will tend to increase the velocities produced in the simulations as compared to those seen in the experiment.

V. CONCLUSION

We have investigated the dynamics of solid plasma created by high-contrast intense laser pulses using pump-probe Doppler spectroscopy. Experimental data shows a rapid outward motion of the probe critical layer at early time. This feature of the data is reproduced by simulations only in the case that there is no pre-plasma formation at the target surface. Such a diagnostic technique is of interest for a variety of applications in which pre-pulse ablation of the target front surface must be avoided to ensure correct target functioning. Optical pump-probe Doppler spectrometry offers a technique that can diagnose plasma formation (or lack there-of) driven by the pre-pulse in a target-surface normal or oblique geometry. Such a geometry is significantly less constraining on other aspects of the experimental design than the side-on imaging techniques usually employed to diagnose pre-plasma formation.

ACKNOWLEDGMENTS

GRK acknowledges J.C. Bose Fellowship grant (JCB-037/2010) from the Science and Engineering Research Board, Government of India. JP acknowledges the support of the Newton-Bhabha Scheme administered by STFC.

[1] R. P. Drake, *High Energy Density Physics* (Springer-Verlag, Berlin, Heidelberg, 2006).

[2] P. Gibbon, *Short Pulse Laser Interactions With Matter* (Imperial College Press, 2005).

[3] G. A.Mourou, T. Tajima, and S. V. Bulanov, Rev. Mod. Phys. **78,** 309 (2006).

[4] L. Yu-Tong., W. Wei-Min, L. Chun and S. Zheng-Ming, Chin. Phys. B **21,** 095203 (2012).

[5] J. Faure, Y. Glinec, A. Pukhov, S. Kiselev, S. Gordienko, E. Lefebvre, J. P. Rousseau, F. Burgy, V. Malka, Nature **431,** 541 (2004).

[6] R. A. Snavely, M. H. Key, S. P. Hatchett, T. E. Cowan, M. Roth, T.W. Phillips, M. A. Stoyer, E. A. Henry, T. C. Sangster, M. S. Singh, S. C. Wilks, A. MacKinnon, A. Offenberger, D.M. Pennington, K. Yasuike, A. B. Langdon, B. F. Lasinski, J. Johnson, M. D. Perry and E. M. Campbell, Phys. Rev. Lett. **85,** 2945 (2000).

[7] Hui Chen, Scott C. Wilks, James D. Bonlie, Edison P. Liang, Jason Myatt, Dwight F. Price, David D. Meyerhofer and Peter Beiersdorfer, Phys. Rev. Lett. **102,** 105001 (2009).

[8] S. C. Wilks and W. L. Kruer **11,** 1954 (1997)

[9] W. L. Kruer, *The physics of laser plasma interactions* (Boulder, Colorado, 2003).

[10] P.Gibbon and E. Forster, Plasma Phys. Controlled Fusion **38,** 769 (1996).

[11] Y. Ping, A. J. Kemp, L. Divol, M. H. Key, P. K. Patel, K. U. Akli, F. N. Beg, S. Chawla, C. D. Chen, R. R. Freeman, D. Hey, D. P. Higginson, L. C. Jarrott, G. E. Kemp, A. Link, H. S. McLean, H. Sawada, R. B. Stephens, D. Turnbull, B. Westover, and S. C. Wilks, Phys. Rev. Lett. **109,** 145006 (2012).

[12] S. Mondal, A. D. Lad, S. Ahmed, V. Narayanan, J. Pasley, P. P. Rajeev, A. P. L. Robinson, and G. R. Kumar, Phys. Rev. Lett. **105,** 105002 (2010).

[13] A. Adak, D. R. Blackman, G. Chatterjee, P. K. Singh, A. D. Lad, P. Brijesh, A. P. L. Robinson, J. Pasley, and G. R. Kumar, Phys. Plasma **21,** 062704 (2014).

[14] S. Fourmaux, S. Payeur, S. Buffechoux, P. Lassonde, C. St-Pierre, F. Martin, and J. C. Kieffer1, Optics Express **24,** 8486 (2011).

[15] M. Shaikh, A. D. Lad, K. Jana, D. Sarkar, I. Dey and G R. Kumar, Plasma Phys. Controlled Fusion **59,** 014007 (2017).

[16] I. Dey, A. Adak, P. K. Singh, M. Shaikh, G. Chatterjee, D. Sarkar, A. D. Lad, and G. R. Kumar, Optics Express **24,** 28419 (2016).

[17] M. Cerchez, R. Jung, J. Osterholz, T. Toncian, O. Willi, P. Mulser, and H. Ruhl Phys. Rev. Lett. **100**, 245001 (2008).

[18] L. M. Chen, M. Kando, M. H. Xu, Y. T. Li, J. Koga, M. Chen, H. Xu, X. H. Yuan, Q. L. Dong, Z. M. Sheng, S. V. Bulanov, Y. Kato, J. Zhang, and T. Tajima Phys.

Rev. Lett. **100**, 045004 (2008).

[19] B. Dromey, M. Zepf, A. Gopal, K. Lancaster, M. S. Wei, K. Krushelnick, M. Tatarakis, N. Vakakis, S. Moustaizis, R. Kodama, M. Tampo, C. Stoeckl, R. Clarke, H. Habara, D. Neely, S. Karsch, and P. Norreys Nat. Phys. **2**, 456 (2006).

[20] F. Wagner, S. Bedacht, A. Ortner, M. Roth, A. Tauschwitz, B. Zielbauer, and V. Bagnoud, Optics Express **22**, 29505 (2014)

[21] M. Roth, T.E. Cowan, M.H. Key, S.P. Hatchett, C. Brown, W. Fountain, J. Johnson, D.M. Pennington, R.A. Snavely, S.C. Wilks, K. Yasuike, H. Ruhl, F. Pegoraro, S.V. Bulanov, E.M. Campbell, M.D. Perry, and H. Powell, Phys. Rev. Lett. **86,** 436 (2001).

[22] D. Neely, P. Foster and A. Robinson, Appl. Phys. Lett. **89,** 021502 (2006).

[23] V. Malka, J. Faure, Y.A. Gauduel, E. Lefebvre, A. Rousse, K.T. Phuoc, Nat. Phys. **4**, 447 (2008)

[24] L. M. Barker and R. E. Hollenbach, J. Appl. Phys. **43,** 4669 (1972).

[25] P. M. Celliers, D. K. Bradley, G. W. Collins, D. G. Hicks, T. R. Boehly, and W. J. Armstrong, Rev. Sci. Instrum. **75,** 4916 (2004).

[26] E Kudeki and G R Stitt Geophysical Res. Lett. **14,** 198 (1987).

[27] A. Benuzzi-Mounaix, M. Koenig, and J. M. Boudenne, Phys. Rev. E **60,** 2488 (1999).

[28] C. Iaconis and I. A. Walmsley, Opt. Lett. **23,** 792 (1998).

[29] Rick Trebino, Kenneth W. DeLong, David N. Fittinghoff, John N. Sweetser, Marco A. Krumbugel, and Bruce A. Richman, Rev. Sci. Instrum. **68,** 3277 (1997).

[30] X. Liu and D. Umstadter, Phys. Rev. Lett. **69,** 1935 (1992).

[31] T. D. Arber, K. Bennett, C. S. Brady, A. Lawrence-Douglas, M. G. Ramsay, N. J. Sircombe, P. Gillies, R. G. Evans, H. Schmitz, A. R. Bell, C. P. Ridgers, Plasma Physics and Controlled Fusion **57,** 113001 (2015)